
Calibration and Uncertainty Analysis for the UC Davis Wind Tunnel Facility

By

Dora Yen
Frank Bräuchle

May 2000

Table of Contents

INTRODUCTION	2
METHODOLOGY	2
<i>Evaluation of the Interaction Matrix.....</i>	<i>3</i>
<i>Uncertainty Analysis Method.....</i>	<i>4</i>
<i>ISO method</i>	<i>5</i>
EQUIPMENT AND SETUP	7
<i>Equipment</i>	<i>7</i>
<i>Alignment Process.....</i>	<i>8</i>
<i>Calibration Process</i>	<i>10</i>
<i>Loading Tips</i>	<i>11</i>
DATA REDUCTION RESULTS	11
VALIDATION PROCEDURE.....	14
UNCERTAINTY ANALYSIS RESULTS.....	15
<i>Elemental Error Sources.....</i>	<i>15</i>
<i>Experimental Uncertainty.....</i>	<i>20</i>
CONCLUSION	21
REFERENCES	22
APPENDIX 1 – UNCERTAINTY ANALYSIS.....	23
APPENDIX 2 – STATISTICAL T-DISTRIBUTION TABLE.....	24
APPENDIX 3 – CALIBRATION AND VALIDATION SETUPS	25

Introduction

To solve aerodynamic design problems nowadays, a combination of experimental, theoretical and computational methods is often used. Although computational methods have greatly improved within the last decade and theoretical models are being further developed, wind tunnel experiments remain an important part of design and validation. Just as computational models need to be validated, the “goodness” of wind tunnel results must be evaluated.

Wind tunnel facilities exist all over the world, so in order to consistently compare data, the quality of flow data for the tunnel must be determined. This often requires a detailed calibration process in which flow features and uncertainties are determined for various tunnel section parameters such as airspeed, pressure variations, disturbances/turbulence, measurement and data acquisition systems. Initial calibrations are usually performed when a new tunnel is installed. Although tunnel section flow conditions do not change significantly from manufacturing baseline, the accuracy of any force and moment balance needs to be checked from time to time.

The purpose of this report is to summarize and document the force-moment balance calibration procedure used for the UC Davis Wind Tunnel. The calibration was completed in March of 2000 by Bryan Feldman, Artie Nathan, Frank Bräuchle and Dora Yen. The calibration results were used in various reports in the same year. Instead of realigning the balance itself, which can take months for a competent crew, an interaction matrix method was applied to verify the interactions of the balance and load cells and to correct for them during the data acquisition process. This process is a faster and more efficient way to do a balance calibration. The methodology will be explained and the calibration procedure will be described.

Methodology

The UCD Wind Tunnel uses an external, six-component, pyramidal balance with six interacting load cells. Traditional calibration methods basically require an alignment of the balance and the load cells in such a way that every load cell reads only one component. Instead a method using an interaction matrix is applied to calibrate the wind tunnel balance.¹

In this report a 2-D calibration process is described. This leads to the simplification that only three components need to be considered in the calibration process:

- Side Force, S (corresponds to lift in 2-D test)
- Drag, D
- Yawing moment, n (corresponds to pitching moment in 2-D test)

The method can be easily extended to include the full 3-D calibration by including all 6 components and generating a 6×6 interaction matrix.

Evaluation of the Interaction Matrix

The underlying principle of the interaction matrix is straightforward. For the pyramidal balance, when applying a “true” load in one direction, on one component, ideally zero readings are desired for the other components. In reality however, non-zero readings result. These readings are interaction readings due to misalignment of the tunnel balance. For example, part of the lift is read as drag.

The three components are loaded over their full ranges and the outputs are recorded using the 16-bit data acquisition system. Nine interaction functions, $S_R(S_L)$, $S_R(D_L)$, $S_R(n_L)$, $D_R(S_L)$, $D_R(D_L)$, $D_R(n_L)$, $n_R(S_L)$, $n_R(D_L)$, $n_R(n_L)$ are derived. The subscript R indicates the load read and the subscript L indicates load applied. These functions are plotted, and any non-linearities are fitted by a best linear approximation that passes through zero (Figure 1).

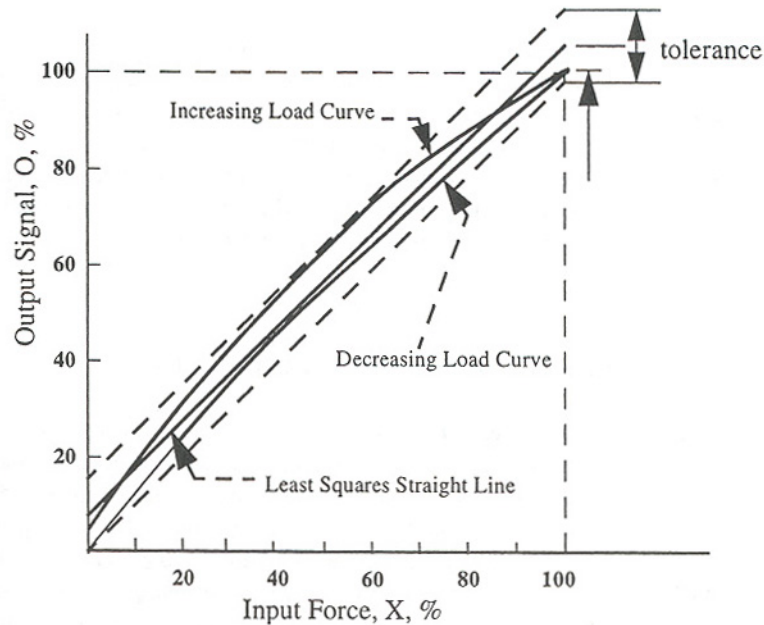


Figure 1. Non-linearities and hysteresis effects.¹

Each loading component is evaluated as a linear combination of the three interacting functions. The result is a linear approximation relating a loading to the reading, where K_{ij} values represent interaction coefficients.

$$\begin{aligned} S_R &= K_{11}S_L + K_{12}D_L + K_{13}n_L \\ D_R &= K_{21}S_L + K_{22}D_L + K_{23}n_L \\ n_R &= K_{31}S_L + K_{32}D_L + K_{33}n_L \end{aligned} \quad (1)$$

Or in matrix form,

$$(F_R) = [K_{ij}] \cdot (F_L) \quad (2)$$

where F represents a force or a moment. By inverting the $[K_{ij}]$ matrix, an expression for the actual loading corrected for interaction effects is derived.

$$(F_L) = [K_{ij}]^{-1} \cdot (F_R) \quad (3)$$

By multiplying the uncalibrated readings $[F_R]$ with the derived interaction matrix $[K_{ij}]^{-1}$, the desired calibrated loadings $[F_L]$ can be obtained.

Uncertainty Analysis Method

A detailed uncertainty analysis is necessary in order to determine the accuracy of experimental results. Data is often analyzed using a standard uncertainty method and presented with a confidence level, typically 95% or 99%. In the past decades, a few methodologies have been developed for uncertainty analysis to standardize and refine the methods used by researchers. In the 1950s, Kline and McClintock⁴ proposed the first method, often referred to as the root-sum-squared (RSS) method, as a means of combining estimated uncertainties. In 1986, an ASME/ANSI Standard was published⁶, which introduced a new method for combining uncertainties. This Standard recommended that uncertainties be divided into two components, systematic (B_j , bias) and random (P_j , precision) as shown in Figure 2. In 1993 the International Organization for Standardization (ISO) published a new ISO Guide (Guide to the Expression of Uncertainty in Measurement⁵). The ISO model is reported to be more consistent in providing uncertainties within prescribed confidence intervals and has become the accepted international experimental uncertainty standard. As a result, uncertainty estimates for results presented are made at a confidence level of 95% based on ISO standards.

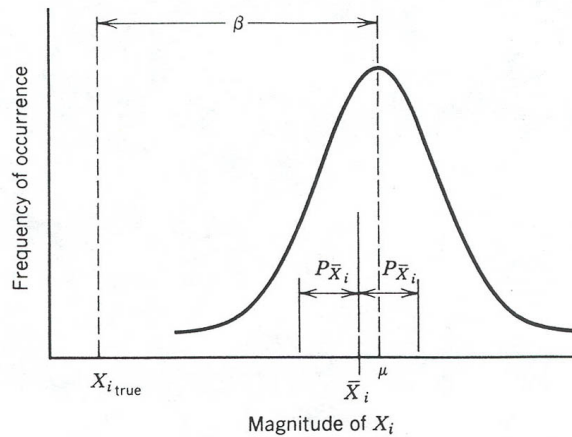


Figure 2. Precision and bias limits about an average sample reading.

P_j represents the precision limit of a sample mean and B_j represents the bias limit. The precision limit, P_j of a sample mean is defined as the interval within which the sample mean, \bar{X} is expected to lie within a desired % confidence. N represents the number of samples. S_j is the precision index of sample population (sometimes called standard deviation) and \bar{X} is the mean of the sample population for that variable.

$$\bar{P} = tS/\sqrt{N} \quad (4)$$

$$S = \left[\frac{1}{N-1} \sum_{i=1}^N (X_i - \bar{X})^2 \right]^{1/2} \quad (5)$$

$$\bar{X} = \frac{1}{N} \sum_{i=1}^N X_i \quad (6)$$

\bar{P}	precision limit of a sample mean
\bar{X}	mean of sample population
S	precision index of sample population or standard deviation
N	number of samples
t	coverage factor from T-distribution table (Appendix 2)

For the results reported, the precision limit is determined by averaging data from multiple tests which reduces the randomness of the errors. For future reference, the “averaging bar” is dropped for convenience and will be simply referred to as P_j .

Bias limit, B_j is an estimated value of the actual bias, β value, within a desired % confidence interval. Since bias terms are fixed errors, averaging multiple tests does not affect the result.

$$\beta \leq B \quad (7)$$

ISO method

The approach is to first estimate the elemental errors and their contribution to the measured variables. A recommended procedure for estimating variable systematic (B_j , bias) and random (P_j , precision) limits follows.

- 1) For an experiment, determine the data reduction equation (DRE) and identify the important variables. Determine how well the final result needs to be known. This will give a guideline how much uncertainty in each variable can be tolerated.
- 2) After identifying the important variables, estimate the range of anticipated test conditions. Next, assume all uncertainties are random at first (precision). Investigate the sensitivity of the uncertainty in the result to the uncertainties in the variables. Focus on the variables whose uncertainties will affect the results the most.
- 3) Concentrate on obtaining detailed estimates of the uncertainties in the most important variables.
- 4) Perform a detailed uncertainty analysis considering systematic (bias) and precision (random) uncertainties. If precise bias and precision limits are unknown, make a reasonable estimate based on the most limiting measurement.
 - a. Usually variables have elemental uncertainty sources, which contributes to its uncertainty. Determine their relative significance first and use an order of magnitude estimate to eliminate insignificant elemental sources. “Rule of thumb for a given variable – those uncertainty sources that are smaller than 1/4 or 1/5 of the largest sources can usually be considered negligible.”².
 - b. Often it is not cost effective or necessary to try to estimate precision limits at the elemental level. These individual elemental uncertainties are often insignificant to the desired result. A more effective approach is to estimate the precision limits of the measured variables at the variable level.

Figure 3 shows how individually measured variables (X_j) are influenced by numerous elemental errors and how these errors propagate into the final result (r).

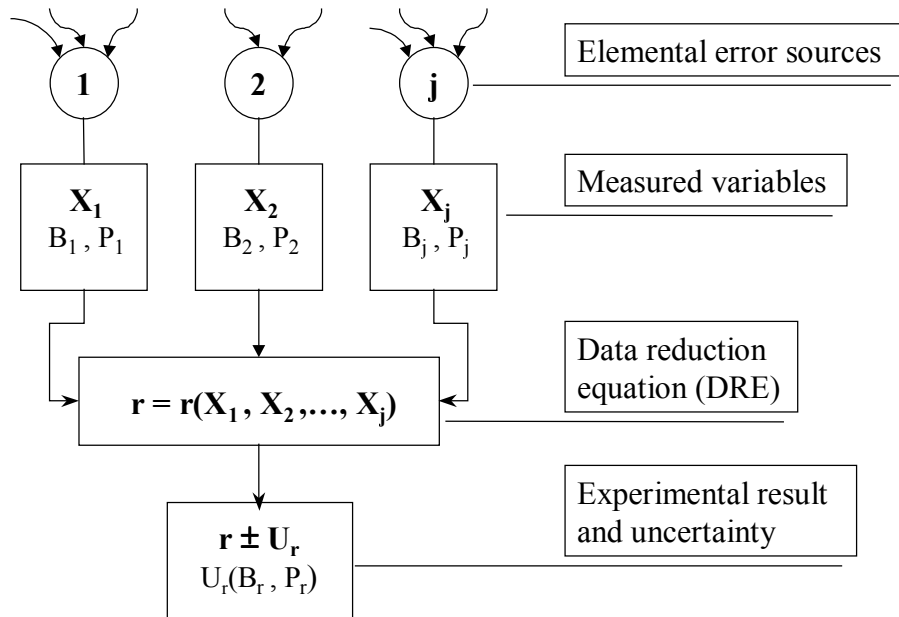


Figure 3. Propagation of uncertainty (B_j , bias and P_j , precision) into experimental results.²

Next, the sensitivity coefficients (θ_j) are determined for each contributing variable (X_j) in the data reduction equation (DRE). The general uncertainty equation for the ISO method is quite extensive and takes into account statistical degrees of freedom associated with estimating the systematic and random uncertainties as well as correlated effects.

$$U_r^2 = \sum_{i=1}^j \theta_i^2 (tb_i)^2 + 2 \sum_{i=1}^{j-1} \sum_{k=i+1}^j \theta_i \theta_k (t^2 b_{ik}) + \sum_{i=1}^j \theta_i^2 (tS_i)^2 + 2 \sum_{i=1}^{j-1} \sum_{k=i+1}^j \theta_i \theta_k (t^2 S_{ik}) \quad (8)$$

Result uncertainty:

$$U_r$$

Bias limit and bias index relation:

$$B_i = 2b_i$$

Precision limit and precision index relation:

$$P = tS / \sqrt{N}$$

Sensitivity coefficients:

$$\theta_j = \frac{\partial r}{\partial X_j}$$

Contributing variable:

$$X_j$$

DRE:

$$r = r(X_1, X_2 \dots X_j)$$

Desired result:

$$r \pm U_r$$

The uncertainty in the result, U_r , is evaluated using a coverage factor, t , corresponding to a confidence level (t is given in a T-distribution table see Appendix 2). S_i and S_{ik} represent the precision indices for individual and correlated effects. Individual and correlated bias indices are expressed as b_i and b_{ij} . For the purposes of this analysis, there are no correlated values, therefore S_{ik} and b_{ij} terms are eliminated.

The Welch-Satterthwaite equation is used to calculate the effective degrees of freedom, v_r , used for determining the t value from a T-distribution table. The v_{S_i} and v_{b_i} are the number of degrees of freedom associated with S_i and b_i .

$$v_r = \frac{\left(\sum_{i=1}^j (\theta_i^2 S_i^2 + \theta_i^2 b_i^2) \right)^2}{\sum_{i=1}^j \left(\left[\frac{(\theta_i S_i)^4}{v_{S_i}} \right] + \left[\frac{(\theta_i b_i)^4}{v_{b_i}} \right] \right)} \quad (9)$$

Due to unavoidable uncertainties in estimating bias and precision uncertainties, determining the degree of freedom is not exact. As suggested by Coleman and Steele, such details seem “excessively and unnecessarily complicated...giving a false sense of the degree of significance.” For use in a majority of engineering tests, they recommend some reasonable approximations to expedite and simplify the analysis process. It is proposed that the error distribution follows a Gaussian and $v_r \geq 9$ be assumed so that a T-table value of $t=2$ can always be used.

These recommendations have been evaluated and are acceptable for use in analyzing the data presented. Considering a 95% confidence level, $v_r \geq 9$, sample size $N_j \geq 10$ qualifies as a “large sample.” (Note, traditionally RSS and ASME required $N \geq 30$ for large sample).

Equipment and Setup

Alignment of cable, pulleys and weight hangers is critical for accurate calibration. This section will list the equipment used and detail the procedures followed for calibrating side force, drag and yawing moment.

Equipment

A listing of equipment used in the calibration is provided in the following equipment list. All calibration equipment is available in the wind tunnel except for the height gauge and the set of calibration weights. The height gauge can be checked out from the Ag Shop and the calibrated weight sets are available from the Civil Engineering Concrete Lab (English and metric units).

ITEM	COMMENTS
calibration rig	front side and back side markers for orientation
pulleys	4 pulleys
center rod	20” long aluminum rod with grooved sections
center rod cap	4 screws on top for locking down cable
side stands	used in yawing moment testing
cables and cable hoops	3/64 inch diameter stainless steel wire, breaking strength 270 lbs
weight hangers	1 lb, 10” hangers from McMaster Carr
calibrated weight set	borrow from concrete lab
18” height gauge	borrow from Ag Shop.

Alignment Process

Centerline markers on the turntable are extended and drawn in on the tunnel floor using fine point markers for more accurate alignment prior to installing the test rig. The calibration rig is placed inside the tunnel test section, as shown in Figure 4. Marks on the rig show the orientation of the rig relative to the wind tunnel (front side vs. backside). Depending on which loading component is to be applied, a different pulley setup is required. Pulleys are attached to the rig and the cable is then treaded around the pulley in the grooves. An one pound hanger is attached to keep the cable taut. Precise alignment of the pulleys, cables and rig is essential in order to ensure “true” loads are applied on one balance component and in the desired direction.



Figure 4. Calibration rig installed in tunnel, side view

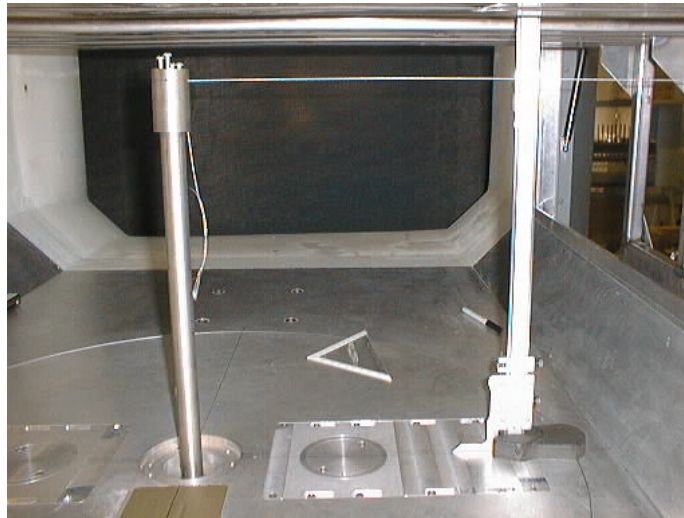


Figure 5. Cable alignment using height gauge and tunnel reference lines.

As shown in Figure 5, the cable and pulleys are aligned vertically and horizontally using an 18” height gauge. By drawing a line perpendicular to the tunnel centerline and aligning the base of the height gauge parallel to the line, cable angularity in the x-y plane (horizontal) can be checked at two points. A point closest to the center rod cap is selected as a reference and the spacing

between the height gauge and the cable is checked at that point. Then the height gauge is moved to a point closest to the pulley and the spacing rechecked. If the spacing does not match the spacing at the reference point, the pulley and cable are adjusted and the process repeated until the spacing at both ends matched. Thus alignment is performed horizontally. The metric scale on the height gauge is used for alignment in the x-z plane (vertical). A two point check is also done near the center rod and then near the pulley to ensure that the cable is level. Figure 6 shows the alignment process using the height gauge.

Once the pulleys and cables are set and aligned and a weight hanger is attached, calibration with weights can begin. Examples of pulley and stand setup for side force, drag and yawing moment are given in Figure 6, Figure 7 and Figure 8. Note in Figure 8, the center rod is removed and the black support struts are inserted. It was determined that the center rod restricted the yawing moment.



Figure 6. Side force pulley and cable setup (left and right setup identical).



Figure 7. Drag pulley and cable setup shown with small weights attached.



Figure 8. Yawing moment pulley, side stands and cable set up. (Note: remove center rod prior to applying loads)

Calibration Process

The calibration procedure is summarized in Figure 9:

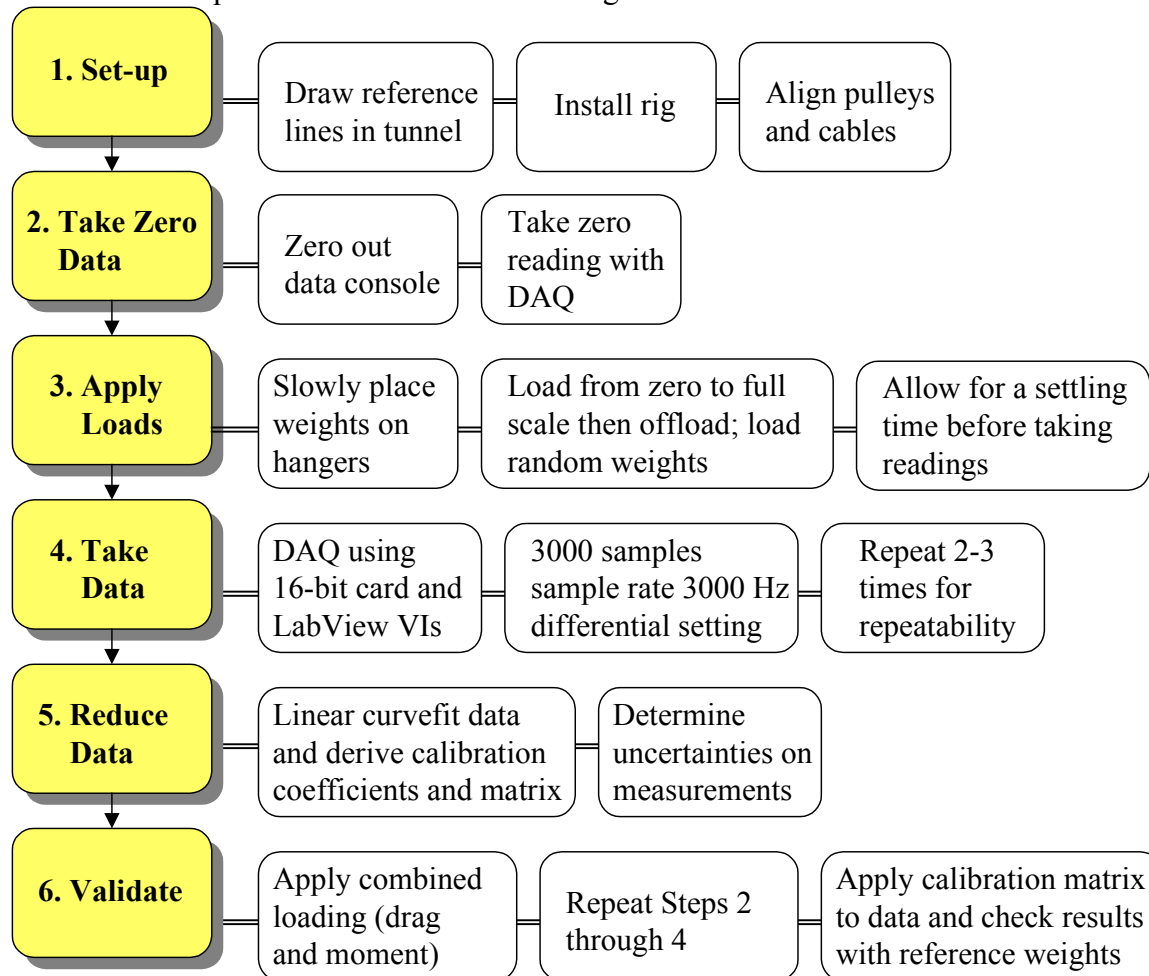


Figure 9. Flowchart showing calibration process.

Loading Tips

Hysteresis effects can be observed by applying loads from zero to full scale then offloading. Random loads are also applied to check the response of the balance without hysteresis. Due to the large loads applied (150 lbs), a settling time is necessary for the load cell to respond.

Application of side force and drag loads is straightforward. However, care must be taken not to bump the hangers or drop the weights onto the hangers. When applying moment loads it is advisable to load the weights on the two pulleys at the same time. This may require three people to perform the test, one on either hanger and one person taking data. All calibration runs should be done several times in order to ensure testing consistency and repeatability.

Data Reduction Results

As previously mentioned, the calibration for the three components S, D, n yields nine functions: $S_R(S_L)$, $S_R(D_L)$, $S_R(n_L)$, $D_R(S_L)$, $D_R(D_L)$, $D_R(n_L)$, $n_R(S_L)$, $n_R(D_L)$, $n_R(n_L)$. Using the side force equation as an example, derivation of the interaction coefficients and the final interaction matrix will be shown.

$$S_R = K_{11}S_L + K_{12}D_L + K_{13}n_L \quad (1)$$

The K_{ij} coefficients are determined as the slopes of the curve fit data, as shown in Figure 10, Figure 11 and Figure 12 (coefficients K_{11} , K_{12} and K_{13} for determining side force). The “Side Force” referred to in the legend is the side force value measured from tunnel instrumentation. This data is electronically corrected via a built-in interaction card, which automatically corrects for interactions; however the amount of correction is not known. The “Side Force wo IC” is the raw data from the balance load cells. A linear curve fit is done on this raw data.

For determining K_{13} coefficient, side force interaction due to applied yawing moment, two distinct slopes result. (Figure 10) Due to different slopes, two values for K_{13} are determined, which results in two interaction matrices. One is valid for positive yaw and the other for the negative yaw. The resulting matrix can easily be incorporated in either the Data Acquisition System or a spreadsheet.

Table 1. Side force interaction coefficients due to drag, side force and yaw loadings.

	K_{11}	K_{12}	K_{13}
Positive yaw	0.96895	0.004	0.01751
Negative yaw	0.96895	0.004	-0.00284

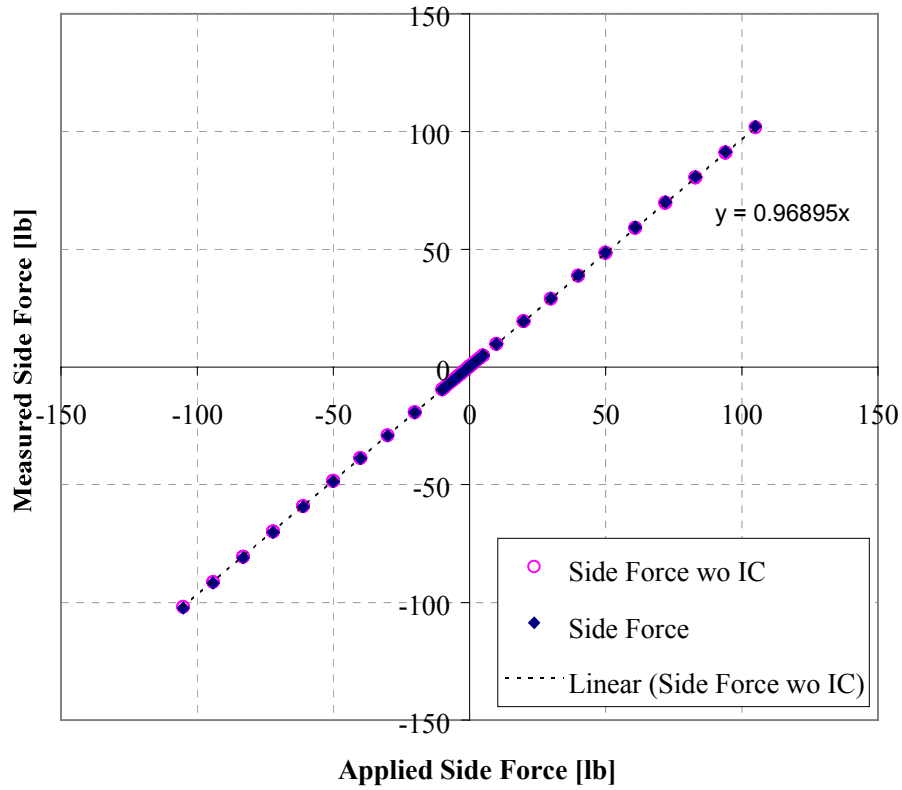


Figure 10. K_{11} , side force coefficient due to side force loading.

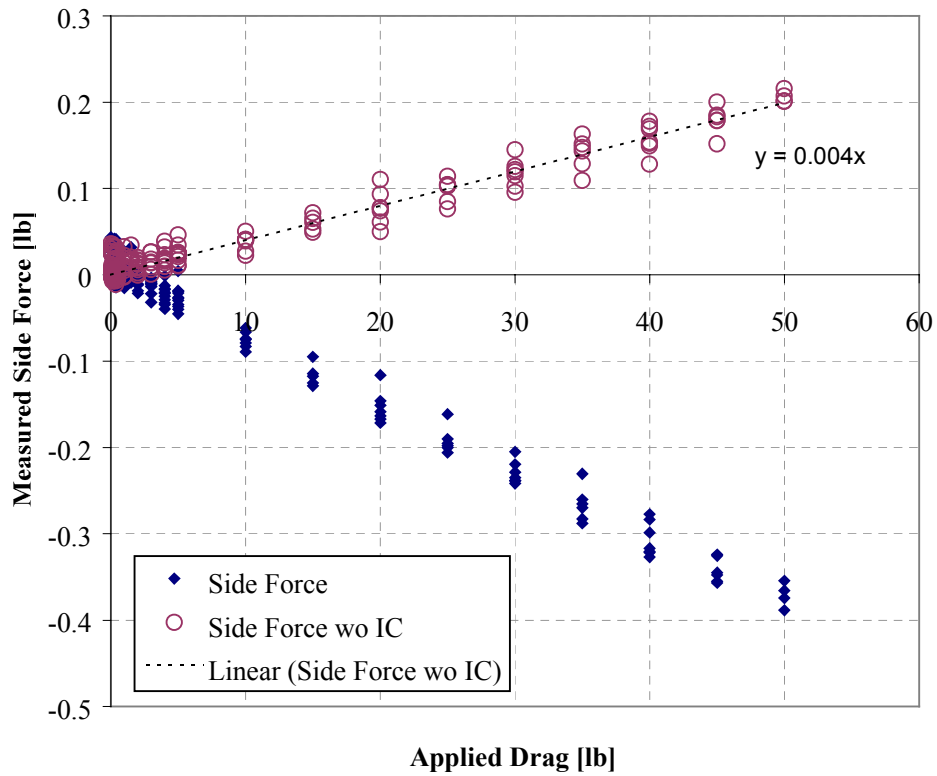


Figure 11. K_{12} , side force coefficient due to drag force loading

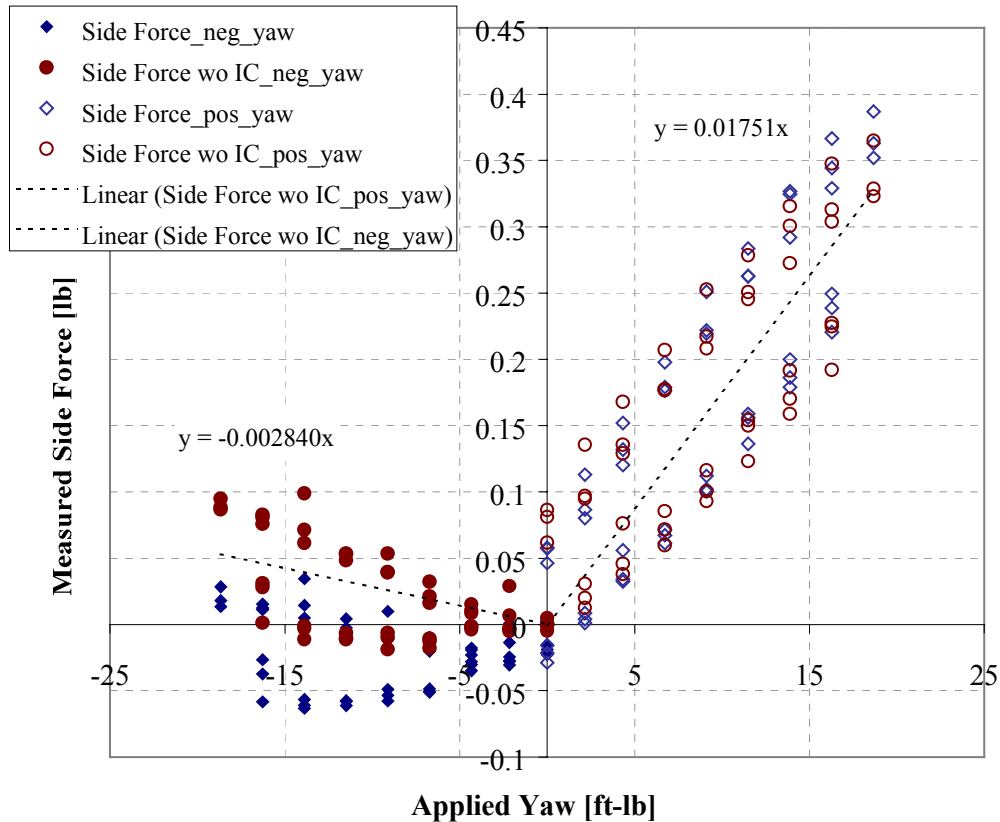


Figure 12. K_{13} , side force coefficients due to positive and negative yaw moment loadings.

The procedure for determining coefficients is repeated for the drag and the yaw functions. Figure 13 shows the two interaction matrices for positive and negative yaw condition, respectively.

$$K := \begin{bmatrix} 0.96895 & 0.004 & 0.0175 \\ -0.0109 & 0.993 & 0.008 \\ 0.00775 & -0.0023 & 0.99299 \end{bmatrix}$$

$$K^{-1} = \begin{bmatrix} 1.03214 & -0.00420 & -0.01816 \\ 0.01139 & 1.00698 & -0.00831 \\ -0.00803 & 0.00237 & 1.00718 \end{bmatrix}$$

Sample Calculation:

read off data: $F_R := \begin{bmatrix} 1 \\ 0 \\ 0 \end{bmatrix}$ loaded: $F_L := K^{-1} \cdot F_R$ $F_L = \begin{bmatrix} 1.03214 \\ 0.01139 \\ -0.00803 \end{bmatrix}$

(a)

$$K := \begin{bmatrix} 0.96895 & 0.004 & -0.00284 \\ -0.0109 & 0.993 & 0.008 \\ 0.00775 & -0.0023 & 0.99299 \end{bmatrix}$$

$$K^{-1} = \begin{bmatrix} 1.03197444 & -0.00415008 & 0.00298493 \\ 0.01139249 & 1.00698474 & -0.00808017 \\ -0.00802787 & 0.00236481 & 1.00701747 \end{bmatrix}$$

Sample Calculation:

$$\text{read off data: } F_R := \begin{bmatrix} 1 \\ 0 \\ 0 \end{bmatrix} \quad \text{loaded: } F_L := K^{-1} \cdot F_R \quad F_L = \begin{bmatrix} 1.03197 \\ 0.01139 \\ -0.00803 \end{bmatrix}$$

(b)

Figure 13. Interaction matrices for (a) positive yaw moment and (b) negative yaw moment along with sample calculations using the matrices.

Validation Procedure

After the evaluation of the final interaction matrices, the results need to be verified by applying combined “true” loads and comparing these with the results obtained with the interaction matrix. The setup for this step can be seen in the Appendix 3.

Figure 14 and Figure 15 show the Δ or deviation in the measured result versus applied load for both the built-in interaction card (w/ IC) and the interaction matrix (w/ matrix). A comparison of these deviation results between the built-in interaction card of the balance and the calibration interaction matrix shows that the UCD calibration yields as good or better results as the interaction card over the range of interest.

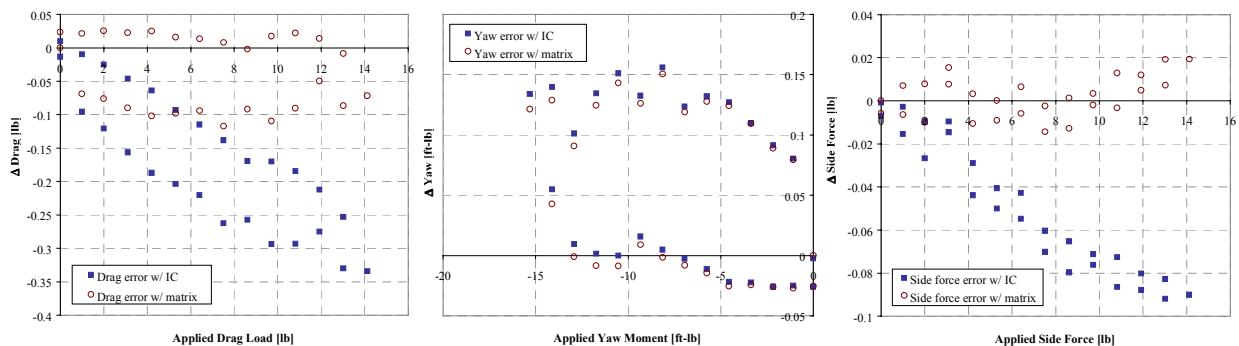


Figure 14. Validation results using negative yaw interaction matrix.

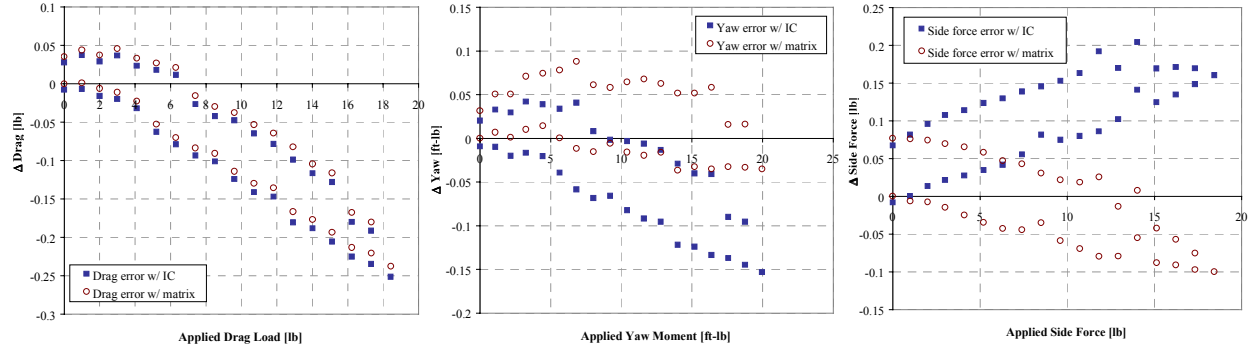


Figure 15. Validation results using positive yaw interaction matrix.

Uncertainty Analysis Results

To calculate c_l , c_d and c_m , the following equations are used. These equations represent the three DREs used for uncertainty analysis, where F_j , U , b , c and k are the important variables.

$$c_l = \frac{kF_{lift}}{\frac{1}{2}\rho U_\infty^2 bc}, \quad c_d = \frac{kF_{drag}}{\frac{1}{2}\rho U_\infty^2 bc}, \quad c_m = \frac{kF_{moment}}{\frac{1}{2}\rho U_\infty^2 bc^2} \quad (10)$$

- F_j = averaged measured loading values
- U_∞ = averaged freestream velocity
- k = correction term
- b = airfoil span
- c = airfoil chord
- ρ = density

Elemental Error Sources

To determine the precision and bias associated with the experimental results an uncertainty analysis is performed on the raw data at the elemental level. Contributing factors to uncertainty include matrix linear curvefitting, resolution of measurement systems and other test condition variabilities. For measurement system uncertainty a frequency analysis is done first on the raw voltage data to ensure that the sampling rate adequately captures the voltage signal from the load cells and transducers. At least a minimum sampling rate based on the Nyquist Criteria would have to be used. From Figure 16, the signal period is about 0.0085 seconds giving a frequency of 120Hz. This high frequency was determined to come from facility power line noise. A sampling rate of 3000Hz is used for data acquisition and more than adequately captures the signal.

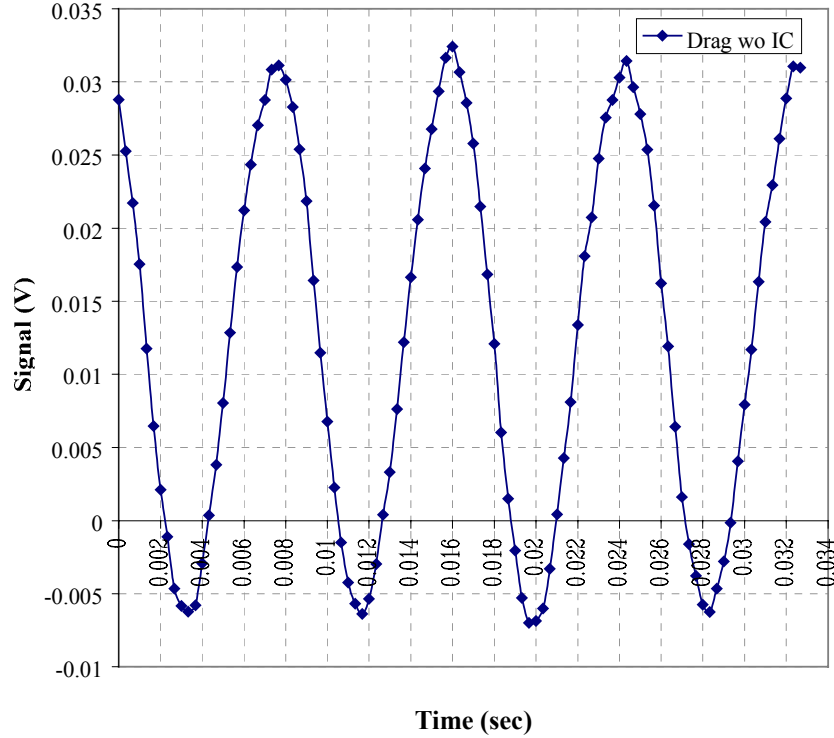


Figure 16. Signal frequency analysis.

Next the resolution of the data acquisition system is determined. A National Instrument AT-MIO16X, 16-bit DAQ card is used for data acquisition. Given a measurement range of $\pm 5V$ (full scale, FS = 10V), the resolution of the card is on the order of 10^{-4} ($2^{16} = 65,536$ bits). With a smaller range of $\pm 2.5V$ (FS = 5V), the resolution is on the order of 10^{-5} (Table 2). The maximum calibration measurements did not exceed 150lbs which is equivalent to $\pm 1.5V$ or FS = 3V. Thus the resolution of the card is determined to be on the order of 10^{-5} .

Table 2. Resolution of DAQ based on full scale values.

Data Range (V)	FS (V)	Resolution (V/bit)
± 1.5	3	4.58×10^{-5}
± 2.5	5	7.63×10^{-5}
± 5	10	1.53×10^{-4}

A total of 3000 time averaged data points are used as the total population. A sample of N=60 points is selected from that population for analysis (Figure 17). Based on standard statistical evaluation methods (assuming Gaussian distribution of data), uncertainty limits within 95% confidence level are determined for each of the load measurements taken. (Table 3)

Table 3. Summary of statistical results for voltage signal data.

	Drag [V]	Side Force [V]	Yaw [V]
Mean	0.01281	0.00591	0.01016
Standard deviation, S_j	1.71×10^{-4}	1.40×10^{-4}	7.68×10^{-5}
Precision limit, P_j	4.41×10^{-5}	3.62×10^{-5}	1.98×10^{-5}

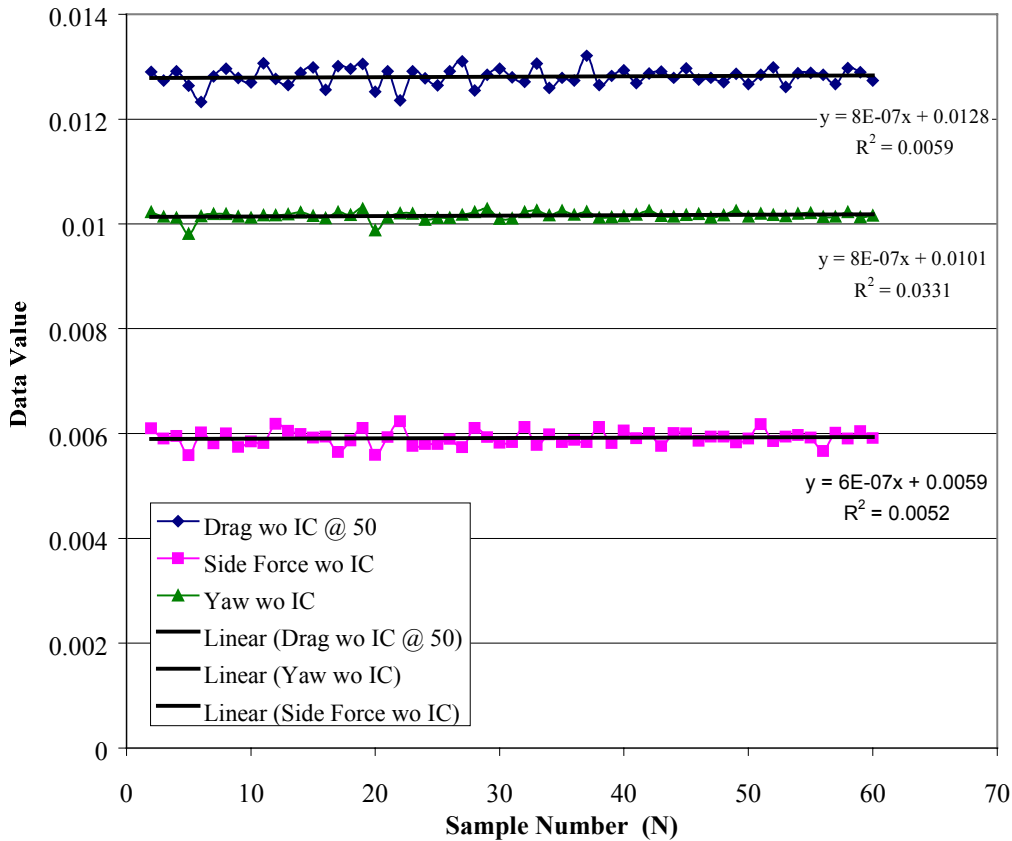


Figure 17. 60 sample data points.

Thus the elemental bias and precision values for measurement system results can now be determined (Table 4). Bias is determined to be the difference between the sample average (60 points) value versus the population average value (3000 points). This represents uncorrectable bias that exists even after applying known offsets. As summarized in Table 5, the bias is on the order of 10^{-6} or approximately machine zero. For evaluation of the data reduction equation (DRE), this bias will be neglected. Although averaged measured values are used, the scatter about the mean cannot be ignored due to the sensitivity of the values measured (i.e., drag). Therefore, precision values are still included and they represent the amount of data scatter about an average. This value is within the resolution expected for a 16-bit A/D card within the FS range tested (10^{-5}).

Table 4. Summary of elemental bias and precision values for force-moment measurements.

	Drag	Side Force	Yaw
Bias	-5.95×10^{-6}	-6.16×10^{-6}	-5.75×10^{-6}
Precision	4.41×10^{-5}	3.62×10^{-5}	1.98×10^{-5}

From the validation results, uncertainty values for data generated using the matrix is determined over multiple tests. The scatter in these tests is quite small, therefore the curvefit uncertainty values determined will be treated as elemental bias values.

Deviation values are plotted as average scatter about zero based on the validation data. Deviation values are given as % of FS loading tested (Figure 18). For loads less than 1.0 lb or ft-lb, refer to Figure 19. Curvefit uncertainty for each loading measurement is summarized in Table 5.

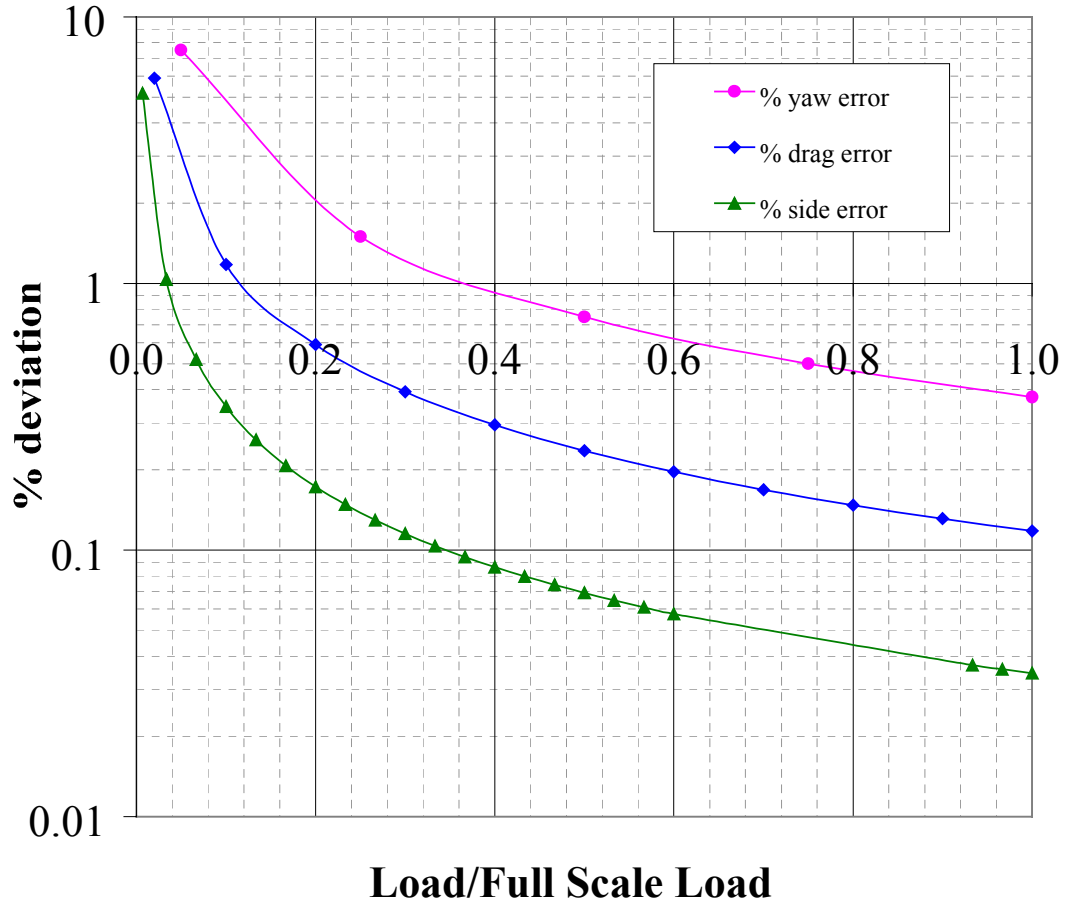


Figure 18. Curvefit uncertainty values for measured load data based on calibration and validation results.

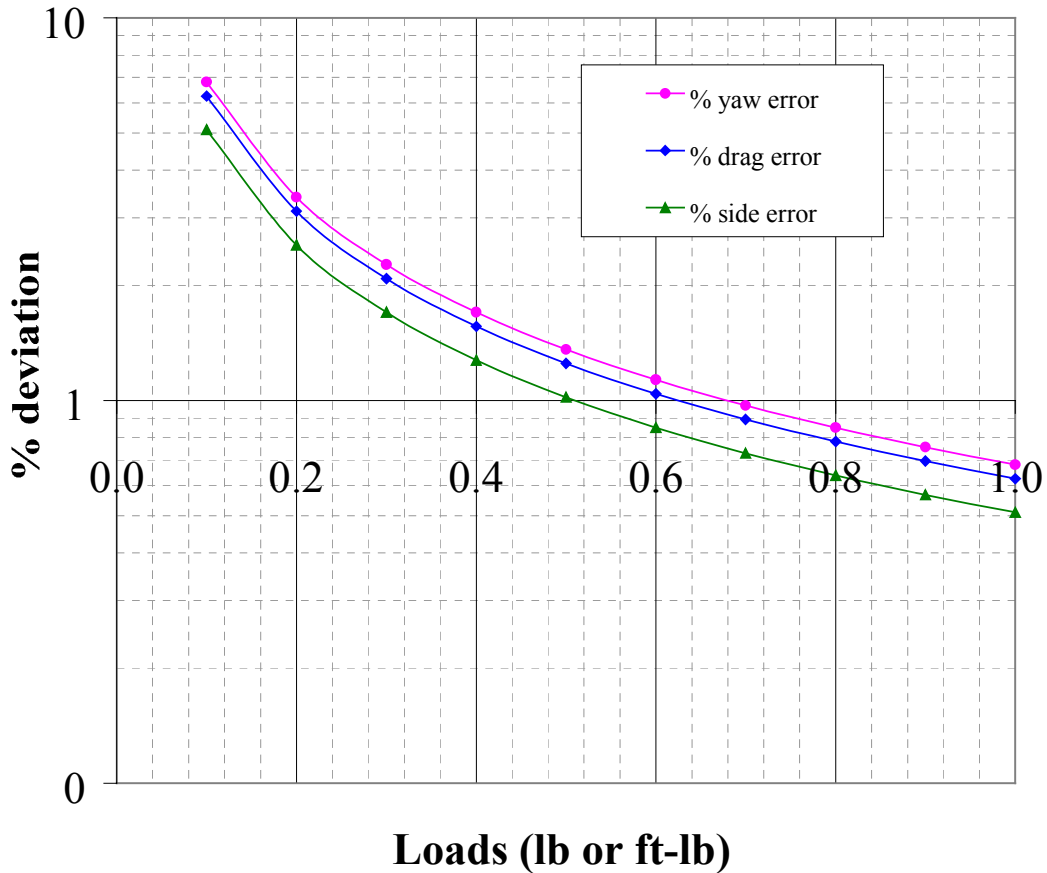


Figure 19. Curvefit uncertainty values for small load ranges (less than 1 lb or 1 ft-lb).

Table 5. Curvefit uncertainty results for FS loads.

Calibration % deviation (loads > 1.0 lb to FS)			
	Drag [lb]	Side [lb]	Yaw [ft-lb]
FS Load	50.00	150.00	20.00
ave +/- %	0.12	0.03	0.38

All other elemental error sources are obtained from manufacturer’s specifications and estimated based on experience using the equipment. Final elemental error sources are summarized and defined in Table 6.

Table 6. Summary of elemental error sources (b_i , S_i) and their descriptions.

Variable	Units	b_1	b_2	b_3	S_1	S_2	S_3
Average F	[lb] or [ft-lb]	0.00004	0.05	0	0.025	0.002207	0
Average U	[mph]	0.1	0	0	0.15	1	0
K	[1]	0	0	0	0.001	0	0
Chord	[in]	0.0015	0	0	0	0	0
Span	[in]	0	0	0	0.01	0	0
Density	[slug/ft ³]	1.16865×10^{-6}	2.22229×10^{-6}	0	0	0	0

Variable	b_1	b_2	b_3	S_1	S_2	S_3
Average F	DAQ resolution 4.41 $\times 10^{-5}$ used (largest value)	data curvefit ± 0.1 lb or ± 0.1 ft-lb estimated	0	scale readability $\pm 0.0005V$	estimated scatter in curvefit	0
Average U	pressure transducer manufacturer specifications	0	0	console controllability ± 0.3 mph	flicker 0.0001V line noise	0
K	0	0	0	± 0.001 results in change in lift coefficient	0	0
Chord	± 0.003 inches from model manufacturer	0	0	0	0	0
Span	0	0	0	± 0.02 inch for scale readability approx. 1/8 inch	0	0
Density	fossilized bias $\pm 0.1\%$	temp variation ± 1 deg F	0	0	0	0

Experimental Uncertainty

Using the ISO equations with some assumptions and appropriate DREs, uncertainty estimates for c_l , c_d and c_m can be determined. (See Appendix 1 for sample calculations.)

Assumptions:

- Gaussian error distributions and degree of freedom ≥ 9 be assumed so $t = 2$ for all cases
- Large sample assumption $N_j \geq 10$
- 95% confidence level
- Correlated values are negligible (i.e., b_{ij} , S_{ij} values are zero)

Table 7 shows typical (lift) values for systematic and random uncertainties along with the sensitivity coefficients. By examining the sensitivity coefficients for each variable and the order of magnitude of the uncertainties, the variable whose uncertainty affects the overall results the most can be determined. Based on the results, that variable is the velocity measurement. By doubling the uncertainties in velocity, the overall uncertainty can change more than 9% whereas doubling uncertainties in force measurements only changes the result by less than 1%. This can be reasoned out since the velocity term is squared in the DRE.

Table 7. Typical lift uncertainty estimates converted to metric units.

Variables	Values	b_j (systematic)	S_j (random)	θ_j , sensitivity coef.
Average F, [N]	274.35471	0.22241	0.111637	0.00254
Average U, [m/s]	49.760444	0.04470	0.452048	-0.02801
K, [1]	0.97	0	0.0005	0.71839
chord, [m]	0.3048	0.000038	0	-2.28621
span, [m]	0.8382	0	0.000254	-0.83135
density, [kg/m ³]	1.2074	0.001294	0	-0.57714

A similar procedure is followed to determine uncertainty estimates for C_d and C_m . Final uncertainty results for C_l , C_d and C_m are summarized in Table 8.

Table 8. Uncertainty estimates for C_l , C_d and C_m .

	C_l	C_m	C_d
U_r	± 0.001	± 0.00005	± 0.000004

Conclusion

A detailed force balance calibration has been completed for the UC Davis Wind Tunnel Facility. Ideally calibrations should be performed prior to each major test. Although this process can be tedious and time consuming, it must be done to ensure the validity of the gathered data. By using an interaction matrix method, the calibration process has been greatly simplified. Uncertainty analysis results for force and moment coefficients show that experimental data measured using the facility is within expected tolerances (within 0.1% for C_l , 0.005% for C_m and within 4% of a drag count for C_d at 95% confidence levels). Based on the analysis, it can also be concluded that variations in velocity due to line noise, temperature variations and other experimental factors must be minimized since this variable most significantly affects the overall results. The procedure followed for calibration, alignment and uncertainty analysis has been documented in this report and will be placed in the Wind Tunnel Facility for future reference.

References

1. Barlow, J.B., Rae, W.H.Jr., and Pope, A., "Low-Speed Wind Tunnel Testing", John Wiley & Sons, Inc., 1999.
2. Coleman, H.W., Steele, W.G., Experimentation and Uncertainty Analysis for Engineers, John Wiley & Sons, New York, 1989.
3. Anon., Guide to the Expression of Uncertainty in Measurement, International Organization for Standardization, Geneva, Switzerland, 1993, ISBN 92-67-10188-9.
4. Kline, S.J. and McClintock, F.A., "Describing uncertainties in single-sample experiments," *Mechanical Engineering* 75(1953), pp.3-8.
5. Guide to the Expression of Uncertainty in Measurement, International Organization for Standardization, Geneva, Switzerland, 1993, p.101.
6. Measurement Uncertainty, ANSI/ASME PTC 19.1-1985 Part 1 ASME, New York, 1986, p. 68.

Appendix 1 – Uncertainty Analysis

Uncertainty Analysis sample calculations for C_m .

Uncertainty Analysis using ISO Standards

(Note: Update values according to the perf coefficient and airfoil used)

Airfoil	UCD 1					
Desired Re Number	1.00E+06 [1]		B1=2b1	b1	manufacturer's, digital flicker equipment bias, fossilized bias	
Chord	12 [inch]	0.3048 [m]		b2	exp curvefit bias	
Span	33 [inch]	0.8382 [m]		b3	TBA	
Area	396 [inch^2]	0.2555 [m^2]	P1=2Si	S1	scale readability	
Density	0.002343 [slug/ft^3]	1.2074 [kg/m^3]		S2	line noise and scatter in multi-test	
Correction K	0.97 [1]			S3	TBA	

		b1	b2	b3	S1	S2	S3
Average M	[lbf-ft]	0.00004	0.05	0	0.025	0.002207	0
Average U	[mph]	0.1	0	0	0.15	1	0
K	[1]	0	0	0	0.001	0	0
chord	[in]	0.0015	0	0	0	0	0
span	[in]	0	0	0	0.01	0	0
density	[slug/ft^3]	1.16865E-06	2.22229E-06	0	0	0	0

		b1	b2	b3	S1	S2	S3
Average M	[N-m]	0.000054232	0.06779	0	0.033895	0.002992251	0
Average U	[m/s]	0.044704725	0	0	0.067057088	0.447047253	0
K	[1]	0	0	0	0.001	0	0
chord	[m]	0.0000381	0	0	0	0	0
span	[m]	0	0	0	0.000254	0	0
density	[kg/m^3]	0.000602291	0.001145314	0	0	0	0

average	average	average	Data from	data points
alpha	M	U		
-2.063383737	25.144275	49.76044405		

Assumptions: Gaussian error distributions and degree of freedom ≥ 9 be assumed so $t=2$ always
 Large sample assumption $N_j \geq 10$ needed only
 95% confidence level desired
 No correlated values

Measurement	Values	b _i (bias)	S _i (precision)	θ_i	$(\theta \cdot b_i)^2$	$(\theta \cdot S_i)^2$
M	25.144275	0.067790022	0.034026822	0.008333	1.27644E-06	3.21597E-07
U	49.760444	0.044704725	0.452048559	-0.008421	5.66951E-07	5.79707E-05
K	0.97	0	0.001	0.216009	0	1.8664E-07
chord	0.3048	0.0000381	0	-1.37486	1.09756E-08	0
span	0.8382	0	0.000254	-0.249975	0	1.61257E-08
density	1.2074	0.001294024	0	-0.173537	2.01711E-07	0
Sum					2.05608E-06	5.84951E-05
					95% U_r	6.05512E-05

Results

	U _{cl}	U _{cd}	U _{cm}	
sample 1	0.0009311	0.0000036	0.000060	within 66-67
sample 2	0.0017672	0.0000049	0.000028	temperature not very well controlled
sample 3	0.0005731	0.0000040	0.000070	within 65-66
sample 4	0.0010837	0.0000046	0.000059	within 66-67, velocity flux
sample 5	0.0017456	0.0000053	0.000032	within 66-67, velocity flux
U_r +/-	0.001	0.000004	0.00005	

Appendix 2 – Statistical T-Distribution Table

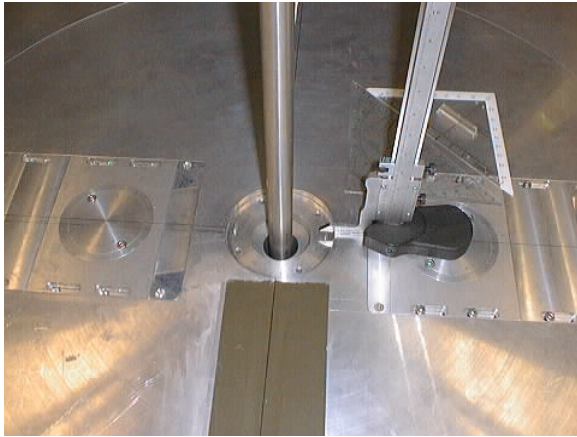
Two-tailed t distribution giving t values for a confidence level C and number of degrees of freedom v.

v	C = 95.0%	C = 99.0%
1	12.706	63.657
2	4.303	9.925
3	3.182	5.841
4	2.776	4.604
5	2.571	4.032
6	2.447	3.707
7	2.365	3.499
8	2.306	3.355
9	2.262	3.250
10	2.228	3.169
11	2.201	3.106
12	2.179	3.055
13	2.160	3.012
14	2.145	2.977
15	2.131	2.947
16	2.120	2.921
17	2.110	2.898
18	2.101	2.878
19	2.093	2.861
20	2.086	2.845
25	2.060	2.787
30	2.042	2.750
60	2.000	2.660
∞	1.960	2.576

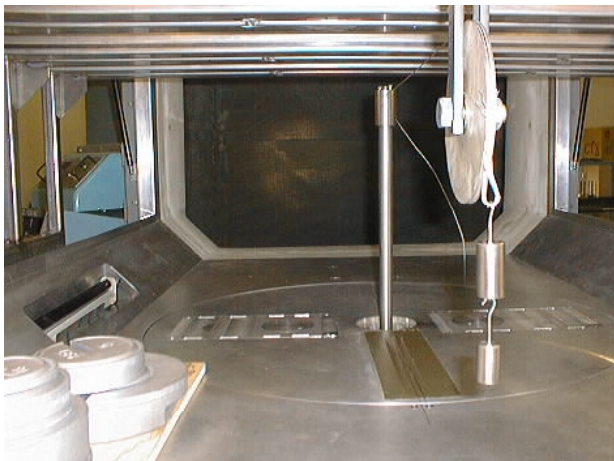
Appendix 3 – Calibration and Validation Setups

Drag Setup

Drag center rod alignment with rod cap and height gauge.

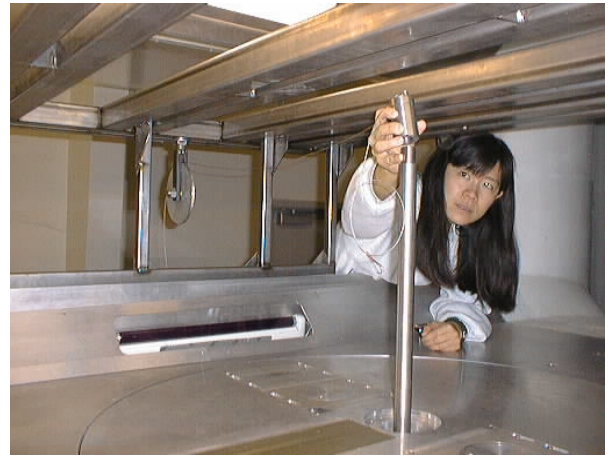


Drag loading with small weights and large weight set. Drag is only loaded in one direction, down the centerline of the tunnel



Side Force Setup

Side force pulley and rod cap set up.

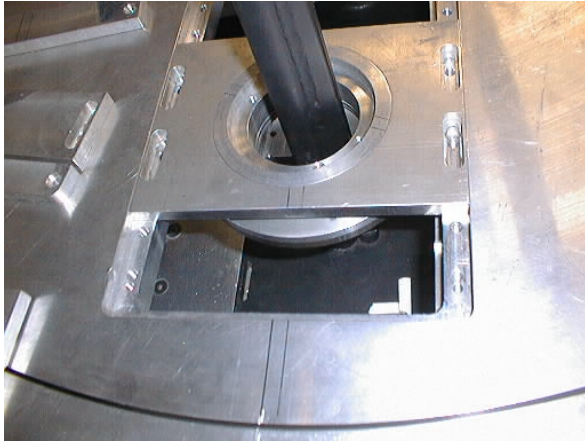


Side force loading is performed outside the tunnel on the left and right sides. Large weights used for full scale loading.



Yaw moment setup

Side stands must be used along with the grooved rod for yaw moment loading.



Pulley installation and alignment of cable in the horizontal and vertical planes.



Left side moment loading shown. Set up for right side loading where pulleys are switched.



Validation Setup

Validation of calibration matrix is performed using a setup similar to the yaw moment loading. In this case, only one pulley is loaded at one time. The other pulley is left unloaded. This results in both a yawing moment and drag applied. Measurements taken are validated against the actual force and moment applied with the weights.

